

4: CHLORINATION OF HIGH TITANIA SLAG

4.2 Calibration of gas rotameters.

4.1: Experimental

The chlorination of oxidised titania slag was carried out using a laboratory scale chlorinator as described before (le Roux, 2001). The schematic diagram is given in Fig.2.5.4a above. The chlorinator consists of a furnace within which a cylindrical silica reactor of 55mm external diameter was inserted. The reactor contained a silica perforated plate in the middle of the tube. A gas mixture of CO, Cl₂ and N₂ (whose flow rates were controlled by three rotameters) was passed through the bed from the bottom of the reactor. A mercury manometer was used to indicate the gauge pressure of the gas flowing into the reactor and a separate mercury manometer was also used to indicate the gauge pressure of the hot gas at the reactor exit. The hot gas mixture flowing out of the reactor was cooled through an off-gas condenser and finally through a scrubber system. The scrubber system consisted of four flasks. The first was empty and was used to collect the solid residues from the system. The second one contained tetrachloromethane which was used to absorb titanium tetrachloride, while the two others contained concentrated sodium hydroxide which absorbed the excess chlorine from the product stream. Tetrachloromethane was used in the second container to avoid water which might react with titanium tetrachloride to form oxychloride which would block the pipes. The inner diameter of the off gas system through the condenser was in the range of 9mm. The flow rates at minimum and maximum fluidization velocities at room temperature were calculated to be 5.7 and 17.84l/min respectively for particle sizes range 425µm-600µm. Detailed chlorination parameters are given in Appendix I.

4.2 Calibration of gas rotameters.

The three gas rotameters were calibrated to determine the relative amount of gases flowing through the reactor. The same procedure was used for nitrogen and carbon monoxide, and another for chlorine.

4.2.1: Nitrogen and carbon monoxide flowrates.

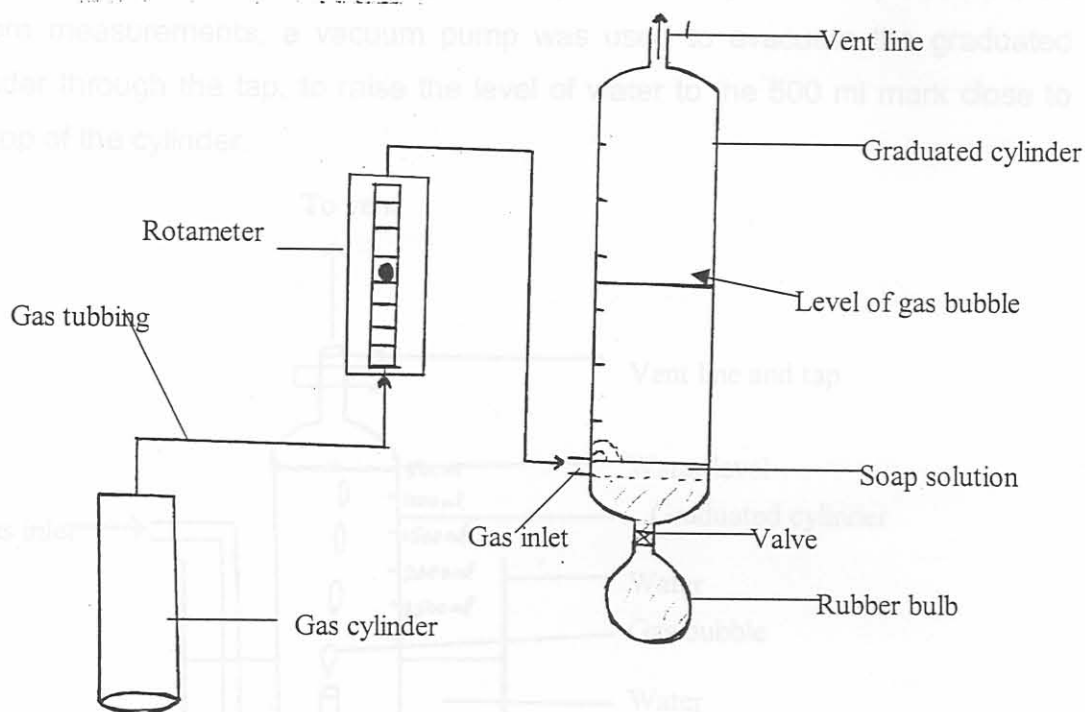


Figure 4.2.1: Schematic diagram of the apparatus used to determine the flowrate of CO and N₂.

The gases were allowed to flow from the regulator on the gas cylinder through the rotameters to a graduated cylinder containing liquid soap. The soap created bubbles which moved upward and exited through the vent line. The flowrates were measured by determining the time taken by the gas bubble to travel through a specific length of the cylinder. From the radius of the cylinder, the volume travelled by the gas during a specific time interval was determined and hence the

flow rate was calculated. The ambient temperature and atmospheric pressure of the laboratory were 22°C and 86kPa respectively.

The rubber bulb was used to increase the level of liquid soap in the cylinder when required.

Unfortunately, this method could not be used with chlorine since the gas reacted rapidly with the soap solution preventing the formation of the gas bubbles. The chlorine flowrate was determined by using the apparatus shown in figure 4.2.2 in which the gas flowing into an upturned graduated cylinder displaced water. Before measurements, a vacuum pump was used to evacuate the graduated cylinder through the tap, to raise the level of water to the 500 ml mark close to the top of the cylinder.

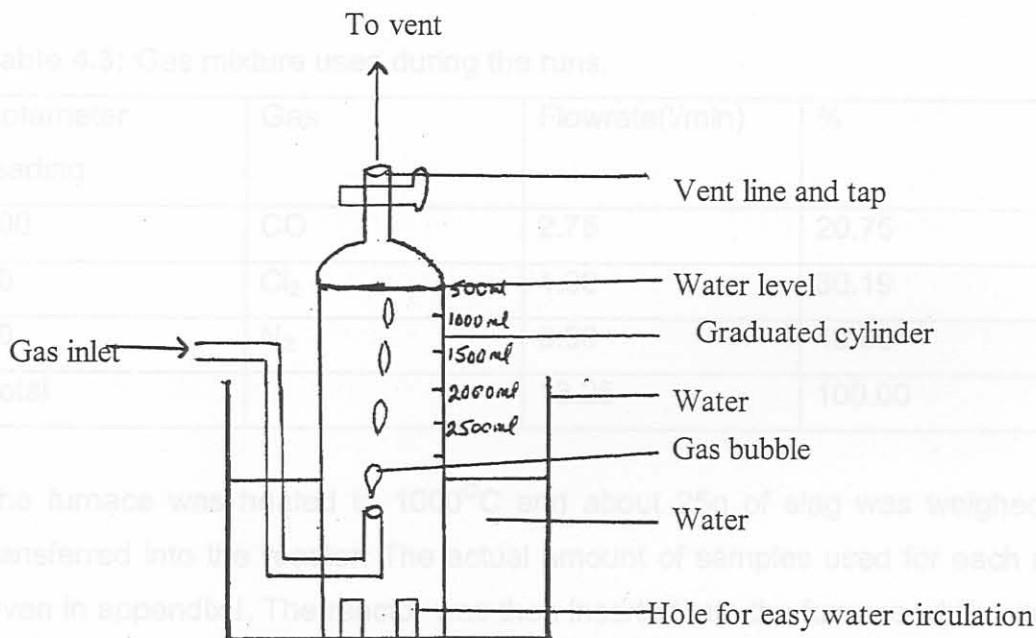


Figure 4.2.2: Schematic diagram of the apparatus used to determine the flowrate of chlorine.

After evacuation, the tap was closed and the tap exit connected to the vent line. The chlorine gas was allowed to flow through the rotameter into the graduated cylinder from below. As the chlorine flowed, the level of water fell; the time taken

for the level to fall from 500 to 1500 marks was recorded. The detailed result for the calibration of the three gases and the flowrate for each rotameter position are given in appendix J

4.3: Experimental Procedure

The following reaction parameters were used during all the runs.

Atmospheric pressure = 86kPa

Total pressure that could be tolerated was in the range 108-115 kPa at a flowrate of 16.5l/min at 22.50°C .

Reaction temperature = 1000°C

The block route slags and granulated slag of size range 1700-2360µm were fragmented to the reaction particle size range of 425µm-600µm.

Table 4.3: Gas mixture used during the runs.

Rotameter reading	Gas	Flowrate(l/min)	%
100	CO	2.75	20.75
20	Cl ₂	4.00	30.19
30	N ₂	6.50	49.06
Total		13.25	100.00

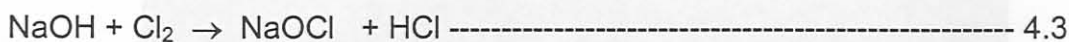
The furnace was heated to 1000°C and about 25g of slag was weighed and transferred into the reactor. The actual amount of samples used for each run is given in appendix I. The reactor was then inserted into the furnace while nitrogen was flowing through at a flow rate of 6.5l/min, which was above the minimum fluidization velocity. When the whole system was gas tight and the temperature at 1000°C, CO and chlorine at flow rates of 2.75 and 4.0l/min respectively were mixed and flowed through the system with the nitrogen. Simultaneously, the stopwatch was started and the time taken for the reaction was recorded. The reaction was repeated for 5, 10, and 15 minutes respectively. At the end of each reaction time, CO and chlorine flows were stopped while nitrogen was allowed to

continue flowing at the same rate to flush the system for at least 5 minutes. The reactor was then disconnected, removed from the furnace and allowed to cool down. The mass of the product was determined (see Appendix I) and samples were collected for SEM, XRD, EDS, WDS and XRF analysis. The temperature rise of the fluidized bed during the first few minutes of chlorination was recorded using a K-type thermocouple. The tips of both the internal and external thermocouples were placed at the centre part of the furnace where the bed is expected to fluidize and the temperature was at 1000°C. The thermocouple within the reactor was enclosed in a silica sheath. The room temperature for each run was also recorded (see Appendix I).

4.3.1: Problems encountered during the chlorination process.

The chlorination reaction proceeded with a lot of difficulties due to blocking of the pipes before and after the sodium hydroxide scrubbers. The pipes before the scrubber were blocked with a mixture of manganese (II), titanium (IV) and iron (III) chlorides. According to (le Roux, 2001), the blocking of the pipes after the NaOH scrubber was due to the formation of $Ti(OH)_4$. These blockages resulted in high back pressure within the system, which tended to force the mercury from the manometers. These blockages were observed to be more pronounced with the block route slag and granulated slag of size range 1700-2360 μ m than with smaller sizes. In other words, for the granulated slag of original size range 425 μ m-600 μ m, the chlorination proceeded smoothly without any problems. The blockage was due to the higher chlorination rates of the first two slags, unlike the slag of smaller sizes (where especially iron oxide was only partially eliminated during initial chlorination). It was also found that the small diameter (9mm) of the off-gas system contributed to the blockage. Redesigning the off-gas system to increase the inner diameter to 14.4mm minimized this problem. The part of the system whose inner diameter could not be increased was washed after each run to minimize blockage. This was done by removing these parts, washing with water then with acetone, drying before assembling for the next run. Replacing the solution in the second scrubber with carbon tetrachloride also prevented the

blockage of the pipe. When all these adjustments were made, the absolute pressure in the system for all the runs was reduced to the range 87.1-96.9 kPa. Finally, white foams were also observed during the runs due to the reaction between sodium hydroxide and chlorine as in equation 4.3.



Foaming appeared to occur when the NaOH solution was saturated with chlorine. The foam also blocked the pipes creating high back pressure in the system.

4.3.2 Optical microscopic examination of the unchlorinated slags.

Optically (under a stereo microscope) the unchlorinated slags appeared black and the intensity of the colour was highest with the unoxidized block route slags as compared to the oxidized slags. The particles of the block route slag and granulated slag of larger sizes (which was crushed before chlorination) were found to be irregular while those of the granulated slag of smaller sizes were more spherical and cylindrical. See Figures 4.3 a, b, and c.

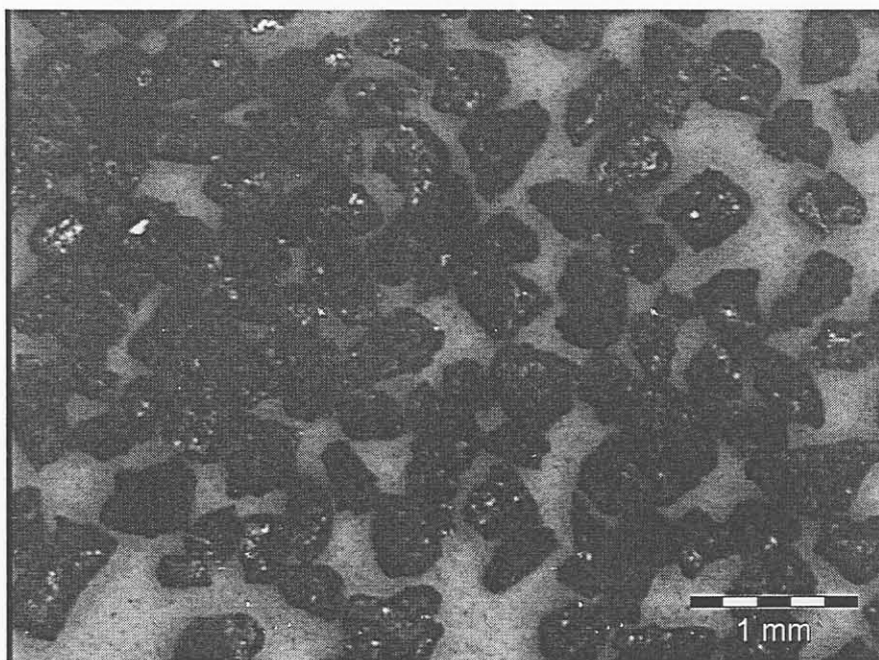


Figure 4.3 a: Optical micrograph of unchlorinated block route slag of the campaign (BSC).

4.4 Results and Discussion.

4.4.1 Optical Micrographs

When the
1700-2360
consists
minutes

g of size
obtained
for 15

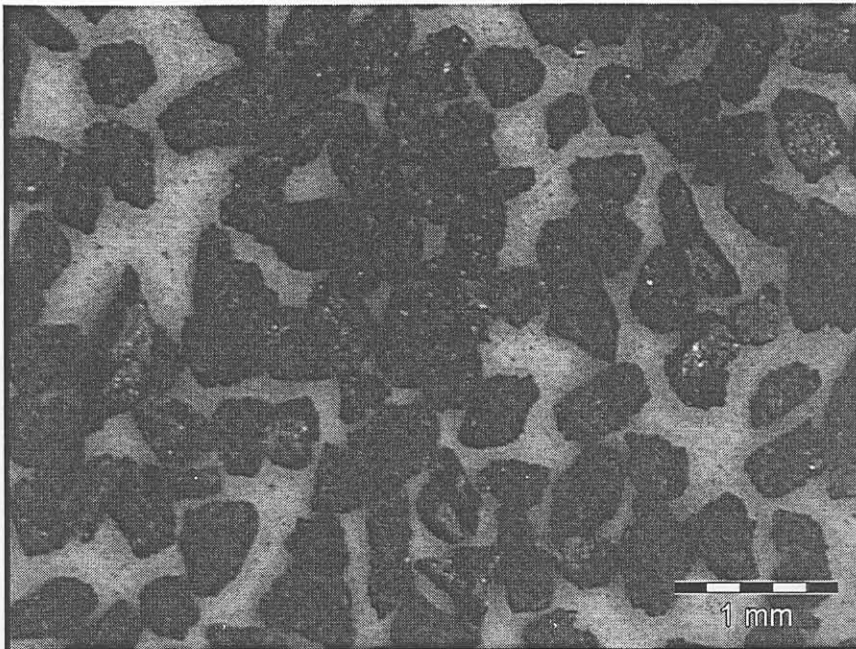


Figure 4.3 b: Optical micrograph of granulated slag of size range 1700 μm -2360 μm after crushing to the size range 425-600 μm , and before chlorination.

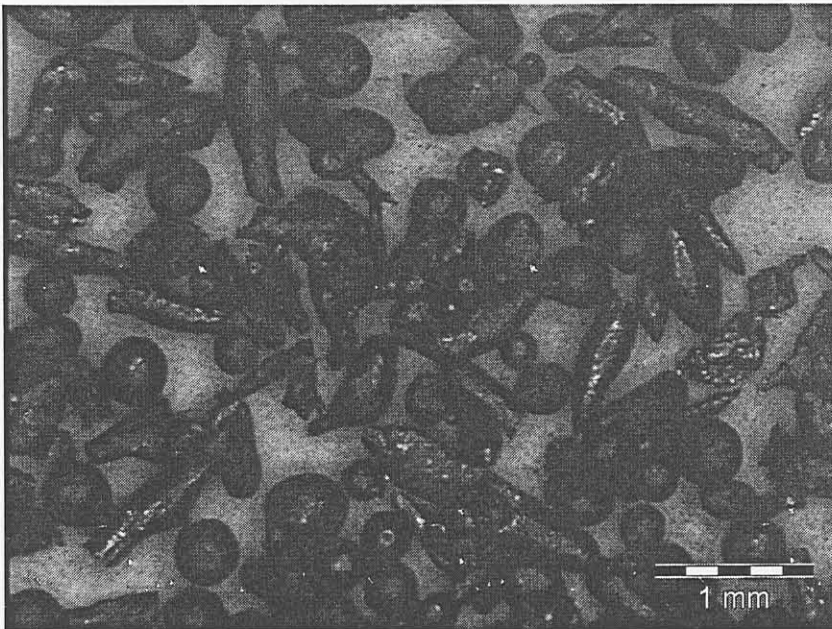


Figure 4.
chlorination

gn (BSC)

Figure 4.3 c: Optical micrograph of granulated slag of size range 425 μm -600 μm .

4.4 Results and Discussion.

4.4.1 Optical microscopic analysis of chlorinated slags.

When the block route slag of the campaign (BSC) and granulated slag of size 1700-2360 μm were chlorinated for 5, 10, and 15 minutes, the product obtained consisted of off-white particles. Optical images of particles chlorinated for 15 minutes are shown in figure 4.4.1 a, and b.

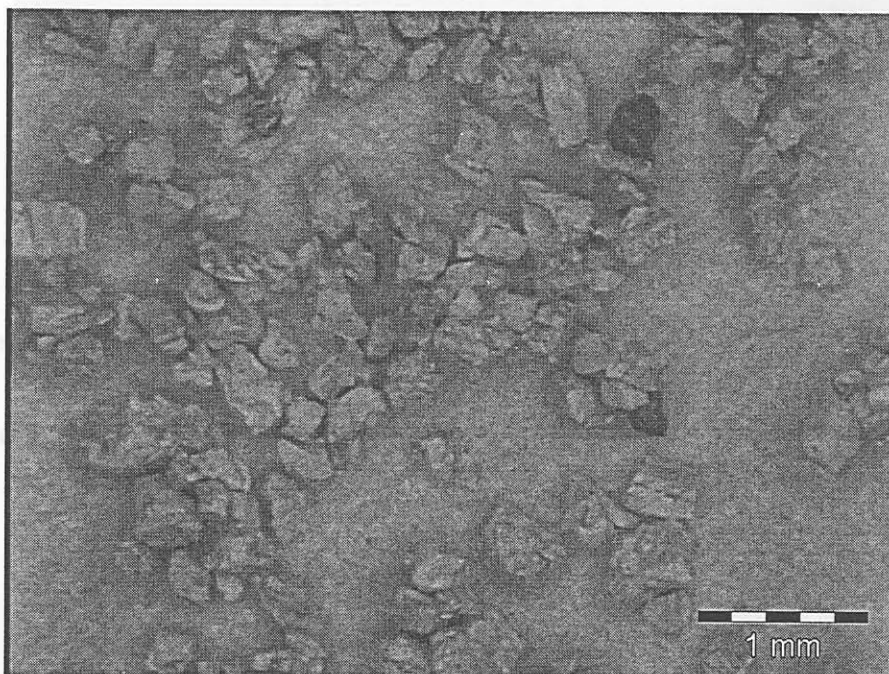


Figure 4.4.1a: Optical micrograph of block route slag of the campaign (BSC) chlorinated for 15 minutes.

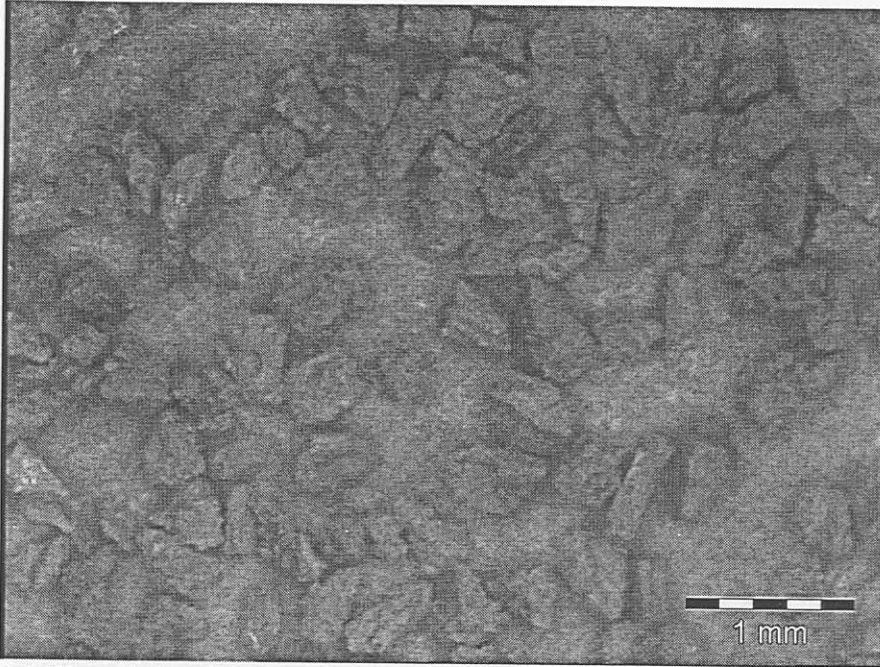


Figure 4.4.1b: Optical micrograph of granulated slag of size range 1700-2360 μm , chlorinated for 15 minutes.

On the other hand, chlorination of the slag of size range 425 μm -600 μm gave a mixture of black and off-white particles, figure 4.4.1 c.

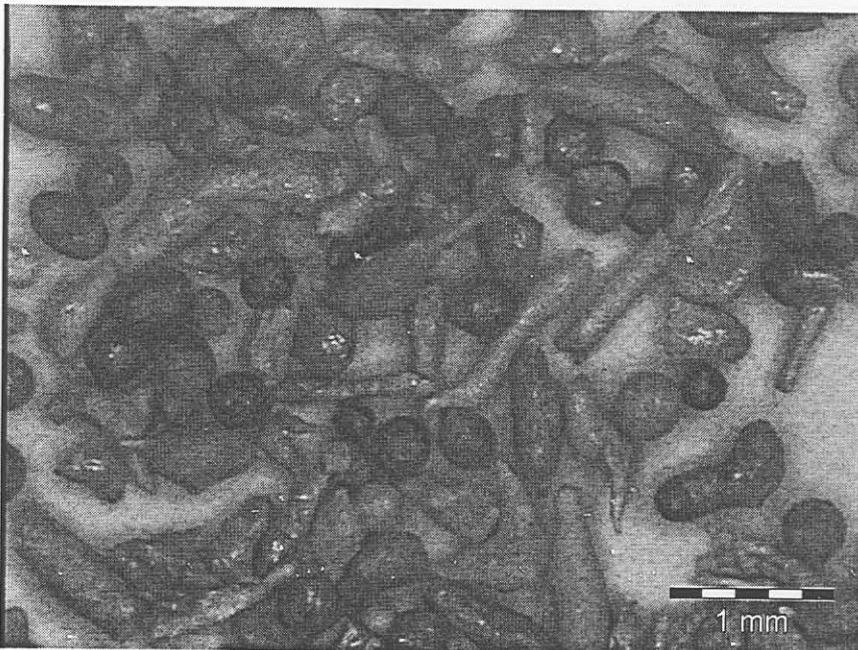


Figure 4.4.1c: Optical micrograph of granulated slag of size range 425 μm -600 μm , chlorinated for 15 minutes.

4.4.2 XRD Analytical Results.

Analysis of the three sets of samples chlorinated for 5, 10 and 15 minutes showed that the products contained a major phase, rutile, with relatively small amounts of ilmenite and pseudobrookite, Appendix G. This result agrees with the XRF results which showed that almost all the MnO and FeO are removed within the first 5 minutes of chlorination, Appendix K. As these impurities were removed, the rutile content increases with chlorination time, Figure 4.6.3 below.

4.4.3: SEM Analytical Result.

The two types of particles obtained after chlorination of the smaller granulated particles ("black and off-white", as shown in figure 4.4.1c) were separated manually, polished and examined by SEM with backscattered electron imaging.

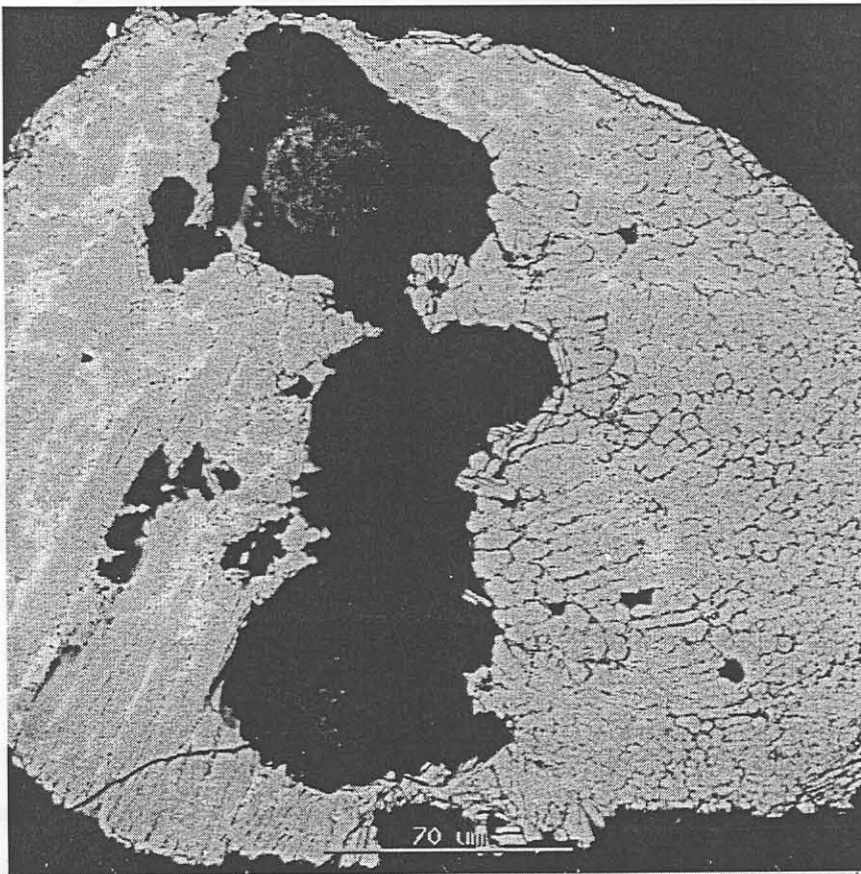


Figure 4.4.3a: SEM micrograph of a black particle of slag of size range 425-600µm chlorinated for 15 minutes .

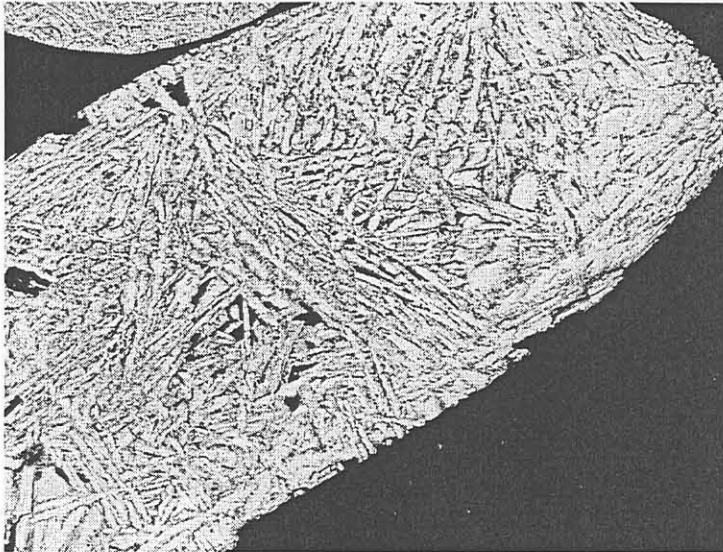


Figure 4.4.3b: SEM micrograph of the light particle of slag of size range 425-600 μm chlorinated for 15 minutes

The SEM micrographs showed that the black particles were smooth, dense with large pores and contain light and dark regions similar to the original slag (Figure 4.4.3a). On the other hand the light particles show a uniformly porous phase with needles of rutile (Fig 4.4.3b).

EDS analysis show that the higher-Z regions of the black particles chlorinated for 15 minutes contained an average of Fe/Ti ratio of 0.37 while the lower-Z regions of these black particles contained an average ratio of 0.04, Appendix E1. On the other hand, the edge and central portions of the light particles also chlorinated for 15 minutes showed a very low content of Fe with an Fe/Ti ratio of 0.007, Appendix E2.

As stated earlier, the chlorinated product of the granulated slag of size range 1700 μm -2360 μm consisted of uniformly off-white particles similar to the light particles above, Figure 4.4.3c.

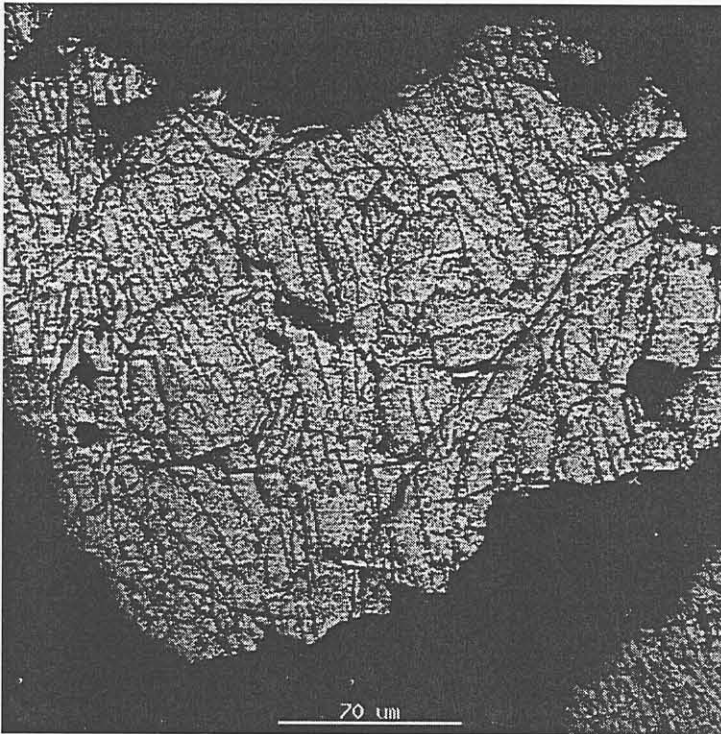


Figure 4.4.3c: SEM micrograph of chlorinated slag of size range 1700 μm -2360 μm chlorinated for 15 minutes.

These results (Figure 4.4.3c) show that, these particles were highly porous and the total porosity was higher than in the case of the slag of size range 425 μm -600 μm , Fig 4.4.3a .

The rutile needles were also observed and EDS analysis confirms that the particles had a very low content of Fe, Appendix E3

Chlorination of block route slag for 5, 10 and 15 minutes also gave uniformly off-white particles, figure 4.4.1a. The chlorinated product was polished and studied using SEM. Results show that the samples chlorinated for 5 minutes consisted of both higher-Z and lower-Z regions. The higher-Z regions were very small and were found close to the centre of the particles while the lower-Z regions of the particles appeared dark, figure 4.4.3d. The higher-Z region were iron-rich and appeared to be unchlorinated M_3O_5 , while the lower-Z outer regions were mainly rutile.

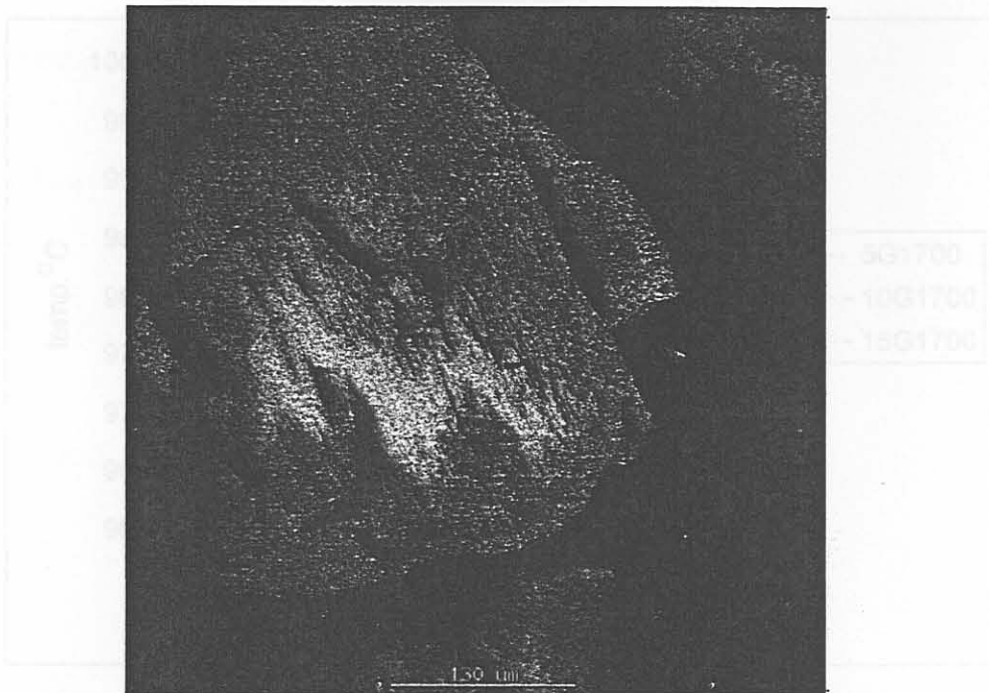


Figure 4.4.3d: SEM micrograph of chlorinated block route slag of the Campaign(BSC) chlorinated for 5 minutes.

EDS analysis of the higher-Z regions show a relatively high Fe/Ti ratio of 0.06 while analysis of the edge gave a very low Fe/Ti ratio of 0.001, Appendix E4.

Generally, the block route slags and granulated slag of size range $1700\mu\text{m}$ - $2360\mu\text{m}$ were more easily chlorinated than those in the size range $425\mu\text{m}$ - $600\mu\text{m}$. This was because the former contained oxides of Fe(II) and Mn(II) that were almost completely chlorinated within the first few minutes of chlorination thereby creating porosity in the particles (see also figures 4.6.1 a and b). This porosity provided a large surface area thereby increasing the chlorination rate for these sets of particles. The slag of size range $425\mu\text{m}$ - $600\mu\text{m}$ consisted of two types of particles. One type contained iron in the +2 oxidation state which chlorinated easily to give the porous off-white particles after the first few minutes of the process. The second type was non-porous due to the presence of iron in the +3 and titanium in the +4 oxidation states which were difficult to chlorinate. These particles remained black (indicative of significant iron) even after 15 minutes of chlorination. The fact that only part of the iron

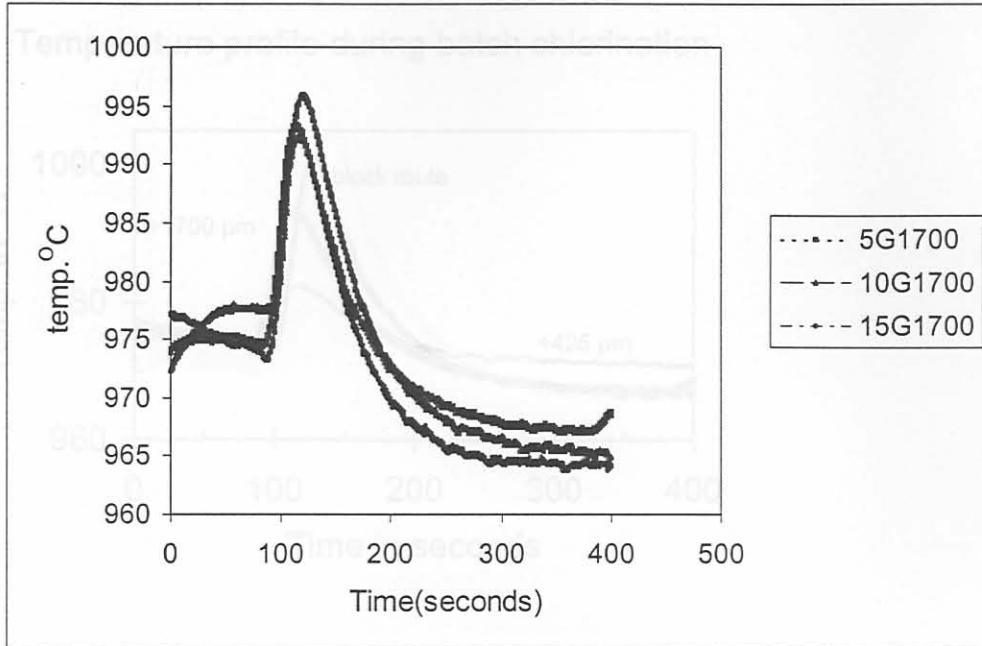


Figure 4.5a Temperature profile during initial chlorination of slag of size range 1700 - 2360 μm , (results from three repeat runs shown).

Pistorius and le Roux, (2002) showed that this temperature increase during chlorination was related directly to the amount of Ti_2O_3 present in the slag. The differences in the temperature changes for the three slag samples shown in figure 4.5b could hence be taken to be related to the levels of FeO , Ti_2O_3 and impurity oxides in the slag. The temperature increased by 30°C for block route slag (BSC), 20°C for slag of size range 1700 - 2360 μm and 8°C for slag of size range 425 - 600 μm reflecting their different Ti_2O_3 contents. During water granulation of the slag, some of the Fe^{2+} and Ti^{3+} were converted to Fe^{3+} and Ti^{4+} respectively. Thus, the amount of Ti^{3+} in the slag decreases in the order 425-600 μm < 1700-2360 μm < BSC; this explains why the heat evolved during initial chlorination decreases in the same order.

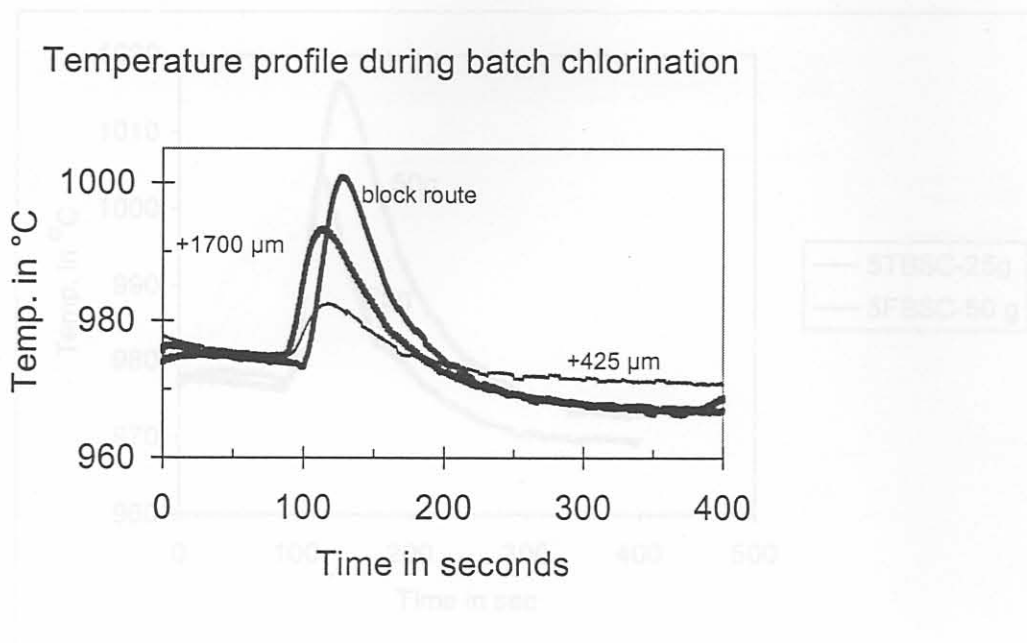


Figure 4.5b: Variation of the temperature change obtained for the initial chlorination of the three slag samples.

Experiments also showed that the temperature increase during the first few minutes of chlorination depended on the amount slag used for each chlorination run. Figure 4.5c shows that, the temperature change when 50g of slag was used was about 18% larger than when 25g of slag was used. This can be explained according to Pistorius and le Roux (2002) to be due to the balance of heat evolution in the volume of the sample with heat lost by radiation from the sample surface, Figure 4.5c.

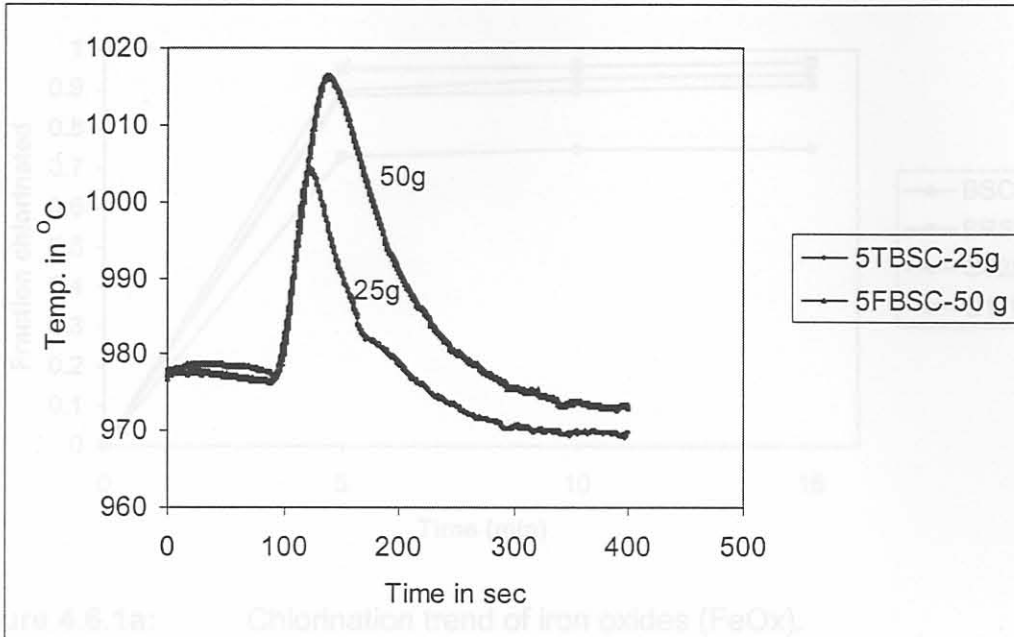


Figure 4.5c: Temperature profile showing the effect of sample mass on reaction exothermicity of the block route slag of the campaign (BSC).

4.6 Initial Rate Of Chlorination

4.6.1 Chlorination rate of FeOx and MnO.

The rate of chlorination of these oxides was comparatively high and the %chlorination of the oxides occurred in the order granulated slag of size range 1700-2360 μm > block route slags > slag of size range 425-600 μm after the first five minutes of chlorination, figure 4.6.1.a and b.

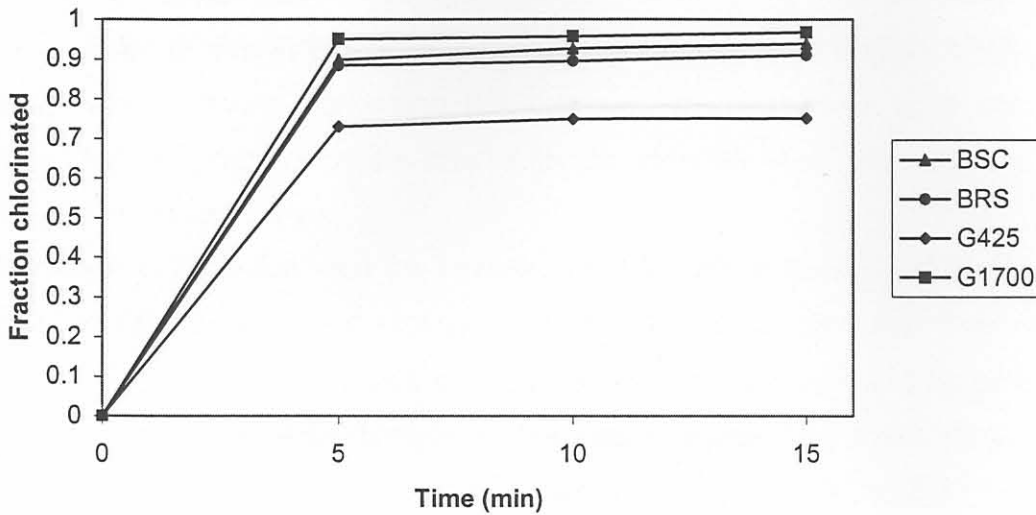


Figure 4.6.1a: Chlorination trend of iron oxides (FeOx). (MnO)

The high chlorination rate of these oxides in the slag of size range 1700-2360 μm could be attributed to the high porosity of the original slag which provides large surface area for the process. This was as compared to the block route slag which was relatively less porous making the initial chlorination of the oxide less rapid. The low rate of chlorination of these oxides in the slag of size range 425-600 μm could be attributed firstly to the fact that, only part of the slag was relatively porous. The non-porous fraction locked some the oxides within the particle preventing them from being chlorinated. Secondly, as revealed by WDS analysis, during water granulation of the slag, almost all the Ti_2O_3 oxidized to TiO_2 while some of the Fe (II) oxides were oxidized to slower reacting Fe (III) oxides.

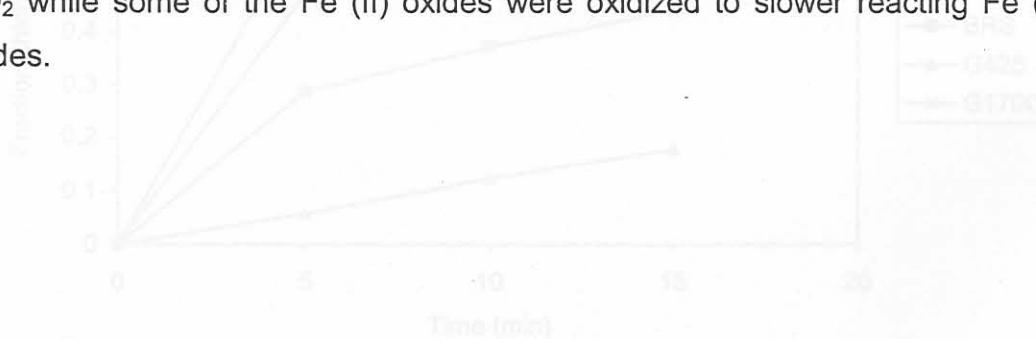


Figure 4.6.2: Chlorination trend of magnesium oxides

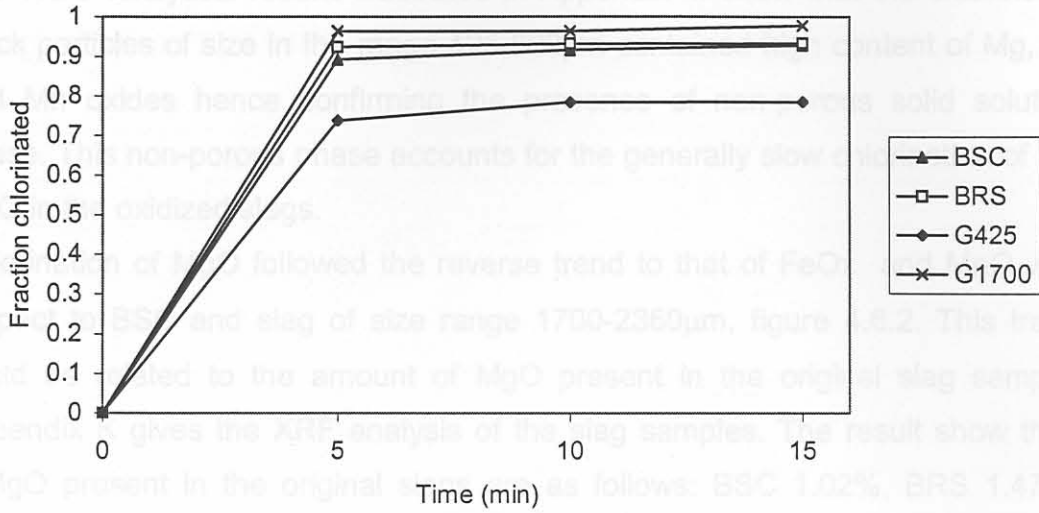


Figure 4.6.1b: Chlorination trend of manganese oxides (MnO).

4.6.2: Chlorination of MgO

As compared to the oxides, FeO and MnO, the chlorination of MgO was slower as only about 5-62% was chlorinated after 5 minutes. The general slow chlorination rate of the MgO phase was due to the association of the high boiling point liquid MgCl₂ with manganese and iron oxides forming a non porous phase.

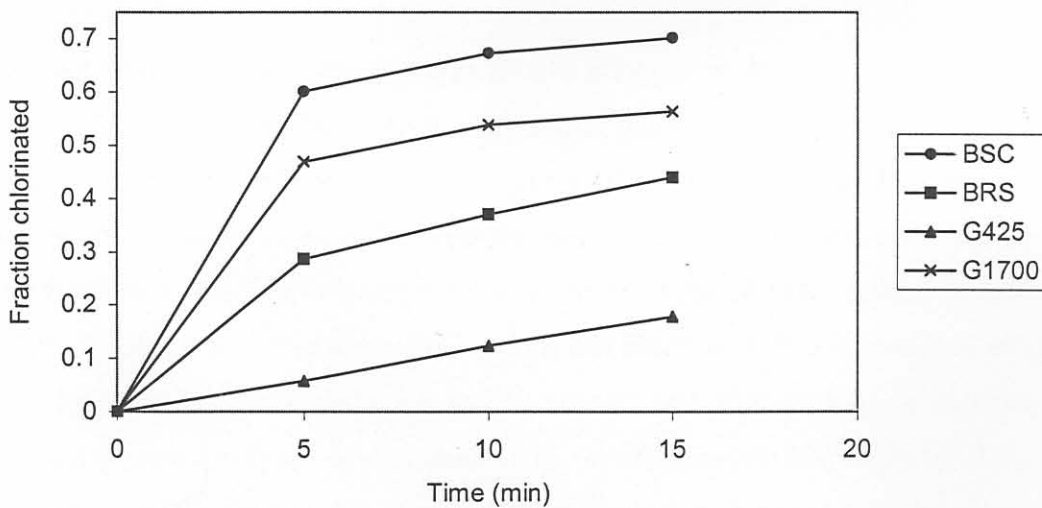


Figure 4.6.2: Chlorination trend of magnesium oxides

The WDS analytical results illustrated in Appendix M show that the chlorinated black particles of size in the range 425-600 μm contained high content of Mg, Fe and Mn oxides hence confirming the presence of non-porous solid solution phase. This non-porous phase accounts for the generally slow chlorination of the MgO in the oxidized slags.

Chlorination of MgO followed the reverse trend to that of FeOx and MnO with respect to BSC and slag of size range 1700-2360 μm , figure 4.6.2. This trend could be related to the amount of MgO present in the original slag sample. Appendix K gives the XRF analysis of the slag samples. The result show that, %MgO present in the original slags are as follows: BSC 1.02%, BRS 1.47%, G425-600 μm 1.06%, G1700-2360 μm 1.11%. The lowest content of MgO in BSC account for the highest chlorination rate of the slag as compared to BRS which contained the highest MgO content. The granulated slag of size range 425-600 μm contained in addition to MgO, Fe (III) and Ti(IV) oxides accounting for the non-porous particles and the lowest chlorination rate observed.

BSC	1.02
BRS	1.47

4.6.3: Chlorination of TiO_2

As stated earlier the oxidation trend of the slags is in the order 425-600 μm > 1700-2360 μm > BSC > BRS. This implies that the percentage chlorination of the titanium dioxide in the slags are expected to decrease in the same order. This might be due to the decrease in porosity and the presence of higher magnesium oxide content in the highly oxidized slags. About 40% of the titanium present in black waste slags is in the form Ti_2O_3 while the titanium in the granulated slag of size range 1700-2360 μm was partially oxidized and that in slag of size range 425-600 μm was completely oxidized. The highest chlorination rate of TiO_2 as exhibited by BSC (Figure 4.6.3) could be attributed to the fact that the slag was unoxidized and contain the lowest amount of MgO. This made it possible for

Table 4.6: Summary of % chlorination of main oxides in titania slag after 5 minutes.

Oxides	Slag type	% Chlorination after 5 minutes.
MnO	G+1700 μ m	96.39
"	BSC	89.25
"	G+425 μ m	73.74
"	BRS	92.40
FeO	G+1700 μ m	95.14
"	BSC	89.83
"	G+425 μ m	72.97
"	BRS	88.37
MgO	G+1700 μ m	46.93
"	BSC	60.10
"	G+425 μ m	5.79
"	BRS	28.68
TiO ₂	G+425 μ m	2.14
"	G+1700 μ m	1.41
"	BSC	3.27
"	BRS	1.48

4.6.3: Chlorination of TiO₂.

As stated earlier the oxidation trend of the slags is in the order 425-600 μ m > 1700-2360 μ m > BSC > BRS. This implies that the percentage chlorination of the titanium dioxide in the slags are expected to decrease in the same order. This might be due to the decrease in porosity and the presence of higher magnesium oxide content in the highly oxidized slags. About 40% of the titanium present in block route slags is in the form Ti₂O₃ while the titanium in the granulated slag of size range 1700-2360 μ m was partially oxidized and that in slag of size range 425-600 μ m was completely oxidized. The highest chlorination rate of TiO₂ as exhibited by BSC (Figure 4.6.3) could be attributed to the fact that the slag was unoxidized and contain the lowest amount of MgO. This made it possible for

most of the FeO and MnO to be chlorinated within the first few minutes hence creating porosity in the slag particles which favours further chlorination.

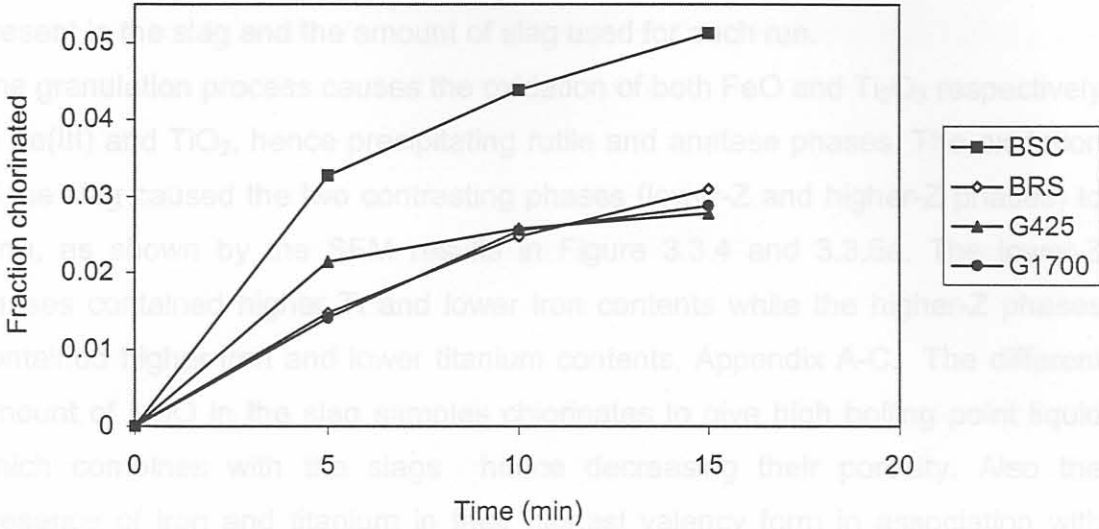


Figure 4.6.3: %Chlorination trend of Titanium dioxides

Comparing the two block route slags, 3.27%TiO₂ and 1.48%TiO₂ from BSC and BRS respectively were chlorinated within the first five minutes. This differences in chlorination rate of TiO₂ for the two block route slags could be attributed to the high MgO content of BRS, Appendix K.

The granulated slags on the other hand are oxidized and contained a relatively small amount of MgO as compared to BRS. Figure 4.6.3 shows that after 5 minutes of reaction time, the % chlorination of TiO₂ in the slag of size range 425-600µm and 1700-2360µm are given as 2.14% and 1.41% respectively. After about 15 minutes of chlorination, the %chlorination of TiO₂ for the typical block route slag (BRS) and the two granulated slags are comparable within experimental error. This show that there is no clear difference between the chlorination rate of block route and granulated slags. Further work, extended to longer chlorination times, would be required to clarify any differences.